RNA METABOLISM

Mixed tailing by TENT4A and TENT4B shields mRNA from rapid deadenylation

Jaechul Lim[1,2]*†, Dongwan Kim[1,2]*, Young-suk Lee[1,2]*, Minju Ha[1,2], Mihye Lee[1,2], Jinah Yeo[1,2], Hyeshik Chang[1,2], Jaewon Song[1,2], Kwangseog Ahn[1,2], V. Narry Kim[1,2]‡

RNA tails play integral roles in the regulation of messenger RNA (mRNA) translation and decay. Guanylation of the poly(A) tail was discovered recently, yet the enzymology and function remain obscure. Here we identify TENT4A (PAPD7) and TENT4B (PAPD5) as the enzymes responsible for mRNA guanylation. Purified TENT4 proteins generate a mixed poly(A) tail with intermittent non-adenosine residues, the most common of which is guanosine. A single guanosine residue is sufficient to impede the deadenylase CCR4-NOT complex, which trims the tail and exposes guanosine at the 3′ end. Consistently, depletion of TENT4A and TENT4B leads to a decrease in mRNA half-life and abundance in cells. Thus, TENT4A and TENT4B produce a mixed tail that shields mRNA from rapid deadenylation. Our study unveils the role of mixed tailing and expands the complexity of posttranscriptional gene regulation.

RNA tailing (nontemplated nucleotide addition to the 3′ end of RNA) is one of the most frequent RNA modifications (*1*, *2*). We previously developed a method called TAIL-seq that reveals the 3′ end sequences of the transcriptome (*3*). TAIL-seq allowed us to investigate the mechanism and function of noncanonical mRNA tailing, such as U tails. Uridylation, particularly oligo-uridylation, occurs selectively on the 3′ ends of deadenylated mRNAs and promotes mRNA decay (*4*–*6*).

Notably, we discovered guanylation at the 3′ termini of mRNAs in HeLa cells, expanding the complexity of mRNA tails (*3*). Unlike U tails, guanylated tails were found mainly among long A tails [≥~25 nucleotides (nt)] and were detected in a form of single-nucleotide addition (Fig. 1A). Guanosine residues were located mainly at the 3′ terminal or penultimate positions (Fig. 1B). Terminal uridine and cytidine residues were found on long A tails, albeit less frequently. Non-adenosine residues in other species—such as mouse, frog, fish, and fly—suggest a conserved modification mechanism (fig. S1A).

Tailing is catalyzed by a group of template-independent nucleotidyl transferases (*7*). Apart from the canonical poly(A) polymerases (PAPs) that cotranscriptionally generate mRNA poly(A) tails, vertebrates have multiple noncanonical PAPs with distinct substrate preferences (fig. S1B). Because some noncanonical PAPs catalyze uridylation instead of adenylation, noncanonical PAPs are also called terminal nucleotidyltransferases (TENTs) (*8*, *9*). To identify the enzyme(s) responsible for guanylation, we conducted TAIL-seq after combinatorial knockdowns of the TENTs. Global guanylation frequency was reduced in TENT4A/4B-depleted (i.e., cells depleted of TENT4A and TENT4B), as well as in TENT1/4A/4B/6-depleted cells (fig. S1, C to E) (*5*). Individual knockdown of TENT4A or TENT4B did not affect guanylation (Fig. 2A), suggesting that these enzymes may act redundantly. Transcript-level analysis indicated that TENT4A and TENT4B may target a substantial fraction of mRNA species (656 out of 901, 72.8%) (Fig. 2B and table S1). A comparable result was obtained with a different set of small interfering RNAs (siRNAs) (fig. S1, E and F). Overexpression resulted in an increase of guanylation (Fig. 2C and fig. S1G), indicating that both TENT4A and TENT4B may catalyze guanylation. Of note, the previous annotation of TENT4A and TENT4B lacked conserved N-terminal extensions that are critical for their activity (fig. S2) (*10*, *11*).

TENT4A (TUT5/PAPD7/hTRF4-1/POLS) and TENT4B (TUT3/PAPD5/hTRF4-2/GLD4) are homologs of yeast Trf4 (*12*). Trf4 was previously shown to catalyze guanylation, but the report has been overlooked owing to the predominant adenylation activity of this protein (*13*). We found in vitro that TENT4B incorporates adenosine triphosphate (ATP) efficiently but also other nucleotides, with a preference for guanosine triphosphate (GTP) over uridine triphosphate (UTP) and cytidine triphosphate (CTP) (Fig. 2D). In vitro incorporation assay with TENT4B and nucleoside triphosphate (NTP) mixtures revealed that G residues were incorporated with a frequency of 15.5%, more than that of U (5.7%) and C (5.2%) residues (Fig. 2E). Consistently, uridylation and cytidylation frequencies decreased in TENT4A/B-depleted cells (fig. S1, H and I). Notably, non-adenosines were distributed without any positional preference at the 3′ terminus (Fig. 2E, bottom right). Similar results were obtained with TENT4A (Fig. 2E, right), indicating that TENT4A and TENT4B generate a mixed tail with a preference for guanosine at irregular positions.

This in vitro result is seemingly inconsistent with our observation from TAIL-seq experiments, which showed a clear positional preference at the 3′ end of poly(A) tails (Fig. 1B). To understand this discrepancy, we investigated whether additional factors are involved in tail remodeling. Deadenylases are 3′-5′ exoribonucleases that favor poly(A) sequences (*14*–*18*). We hypothesized that deadenylase(s) may trim down the mixed tail and stall at non-A residues, thereby exposing non-A at the 3′ terminus. The CCR4-NOT (CNOT) complex is the main cytoplasmic deadenylase complex and has two catalytic subunits: a Caf1 homolog (CAF1a/CNOT7 or CAF1b/CNOT8) and a Ccr4 homolog (CCR4a/CNOT6 or CCR4b/CNOT6L) (*19*, *20*). When immunopurified CNOT7 proteins were incubated with synthetic poly(A) RNAs with intermittent Gs (A50G) (Fig. 3A), a ladderlike pattern was detected at the penultimate position (Fig. 3B, orange arrowheads). The same assay with catalytic mutants showed no ladderlike accumulation (fig. S3A). CNOT6L sheared the adenosine sequences but stalled at each G residue, yielding G at the 3′ terminus (Fig. 3C, red arrowheads). Similarly, C and U residues were able to expose the non-adenosine residues (fig. S3B). Thus, the CNOT complex trims the mixed tail to generate a poly(A) tail with a terminal or penultimate non-adenosine residue.

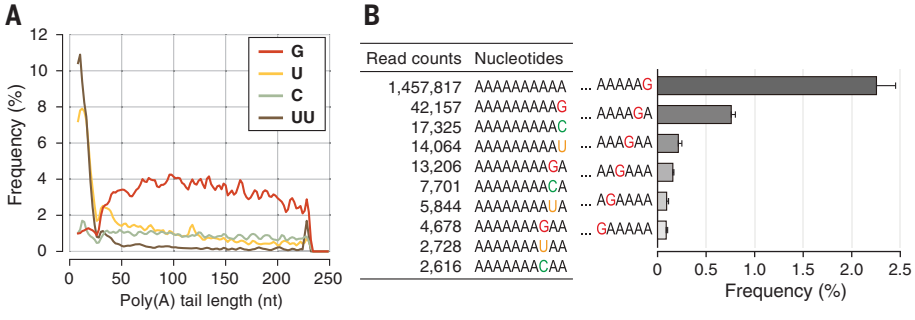

Fig. 1. Pervasive 3′ end guanylation of the poly(A) tail. (**A**) Omnipresent 3′ end guanylation across poly(A) tails of length ≥25 nt. (**B**) Abundant guanosine residues at the 3′ end of the poly(A) tail. (Left) The most abundant 3′ 10-nucleotide sequences. (Right) Terminal and internal guanylation frequencies (n = 4 TAIL-seq experiments). Error bars represent SEM.

[1]Center for RNA Research, Institute for Basic Science, Seoul 151-742, Republic of Korea. [2]School of Biological Sciences, Seoul National University, Seoul 151-742, Republic of Korea.
*These authors contributed equally to this work.
†Present address: Department of Immunobiology, Yale University School of Medicine, New Haven, CT 06510, USA.
‡Corresponding author. Email: narrykim@snu.ac.kr

These results also indicate that even a single non-adenosine residue can counteract deadenylation and stabilize mRNA. Indeed, in vitro deadenylation was substantially delayed in the presence of a single terminal G (Fig. 3D, left, and fig. S3, C and D). Likewise, 3′ penultimate or internal G was sufficient to impede deadenylation (Fig. 3D, right, and fig. S3, D and E). Consistently, the poly(A) tail length of mRNA was reduced in TENT4A/B-depleted cells (fig. S4A). Transcripts with statistically high guanylation were affected more strongly than those with low guanylation (fig. S4B), supporting our hypothesis that guanylation delays deadenylation.

To further examine whether TENT4A and TENT4B have a positive impact on mRNA stability, we performed RNA sequencing in TENT4A/B-depleted cells. A modest transcriptome-wide decrease in mRNA levels was observed (Fig. 4A and fig. S4C and table S2). Transcripts with statistically high guanylation were reduced compared with those that have low guanylation (Fig. 4B and table S3). Another siRNA set produced similar results (fig. S4D). mRNAs with frequent mixed tailing (including G, U, and C) were also destabilized (fig. S4E), consistent with our in vitro deadenylation experiments with non-adenosine residues (fig. S3B). Highly guanylated genes were destabilized in TENT4A/B-depleted cells after actinomycin D treatment (Fig. 4C), indicating that TENT4A/B-mediated mixed tailing may stabilize mRNAs.

Notably, transcripts encoding secreted proteins are frequently guanylated, suggesting an association between mixed tailing and endoplasmic reticulum–mediated translation (table S3). Conversely, many genes involved in protein synthesis (such as ribosomal proteins and translation factors) are not guanylated frequently, indicating that their mRNAs are immune to TENT4A/B-mediated regulation. Highly guanylated mRNAs have longer 3′ untranslated regions (3′UTRs) (fig. S4F), suggesting that the specificity of TENT4A and TENT4B may reside in the 3′UTR. Our motif search did not reveal a particular motif enriched in the UTR, possibly because multiple elements may contribute in combination. TENT4B was previously reported to adenylate and destabilize miR-21 (*21*), but neither an increase in miR-21 level nor a significant change in microRNA (miRNA) targets was found in TENT4A/B-depleted cells (fig. S5). TENT4A/B homolog Trf4 is a component of the TRAMP (Trf4/Air1/2/Mtr4) complex (*22*–*26*), but guanylation was not reduced in MTR4-depleted cells (fig. S6). The results suggest that TENT4A and TENT4B regulate mRNA levels in a miRNA- or TRAMP complex–independent manner.

To measure the impact of mixed tailing on mRNA stability, we performed reporter tethering experiments (Fig. 4D, left). The canonical PAP that selectively incorporates adenosine was used as a negative control for the intrinsic adenylation activity of TENT4A (fig. S7A). Protein and mRNA levels were up-regulated when the reporter was tethered to wild-type TENT4A but not to its mutant (Fig. 4D, right, and fig. S7B). Similar effects

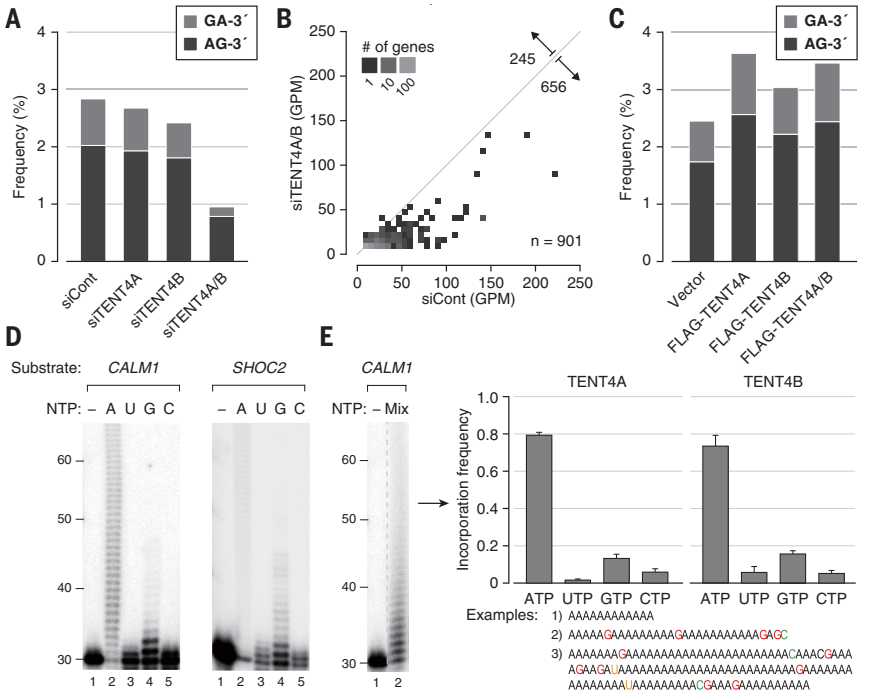

Fig. 2. TENT4A and TENT4B are responsible enzymes for guanylation. (**A**) Decrease in guanylation after knockdown of TENT4A and TENT4B. (**B**) Transcriptome-wide decrease in guanylation after TENT4A and TENT4B knockdown. GPM (guanylated tags per million) was calculated for each transcript. Transcript-level GPMs >3 before or after knockdown of TENT4A and TENT4B were illustrated as a two-dimensional density plot. Cont, control. (**C**) Increase in guanylation upon overexpression of TENT4A and TENT4B. (**D**) In vitro incorporation assay with individual NTP and FLAG-TENT4B. (**E**) In vitro incorporation assays with mixed NTPs showed intermittent guanylation. (Left) In vitro assays with FLAG-TENT4B. "Mix" refers to an NTP mixture (ATP:UTP:GTP:CTP) of 1:1:1:1 ratio. A dashed line shows discontinuous lanes from the same gel. (Right) Extended tails by TENT4A and TENT4B were sequenced by Sanger sequencing (n = 28 and 15, respectively). Error bars indicate SEM.

Fig. 3. Stalled deadenylation of CNOT7 and CNOT6L leads to the accumulation of guanosine at the 3′ end. (**A**) Illustration of RNA substrates. Guanosine residues are colored in red, and distances (in nucleotides) from the 5′ end are labeled. Red and orange arrowheads denote the 3′ end of G and the subsequent A (GA), respectively. (**B**) In vitro deadenylation assay with FLAG-CNOT7. (**C**) In vitro deadenylation assay with FLAG-CNOT6L. Asterisks mark chemical artifacts from oligonucleotide synthesis. (**D**) In vitro deadenylation assays with A20, A19G (left), or A18GA (right) substrates and FLAG-CNOT7. The relative abundance of intact RNAs (of length 20 nt) was compared by mean estimation and SEM error bars (n = 3).

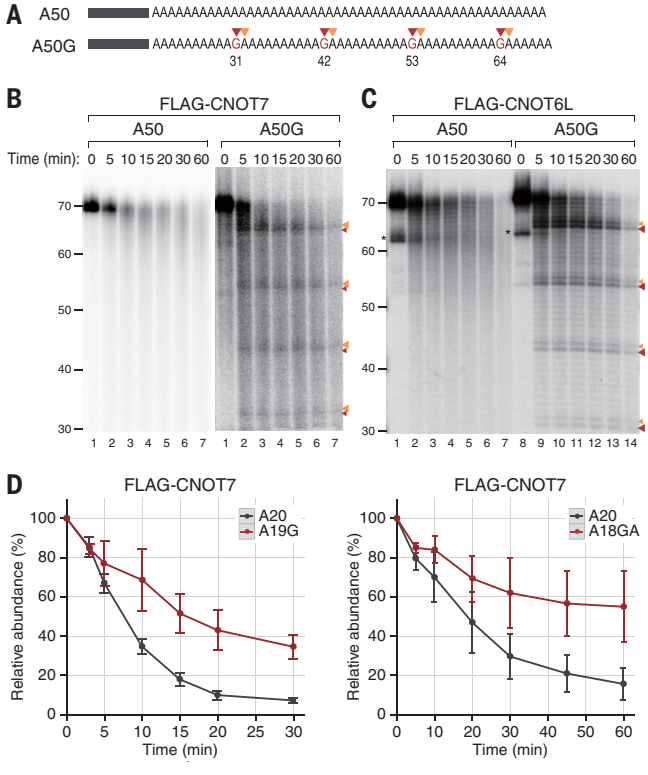

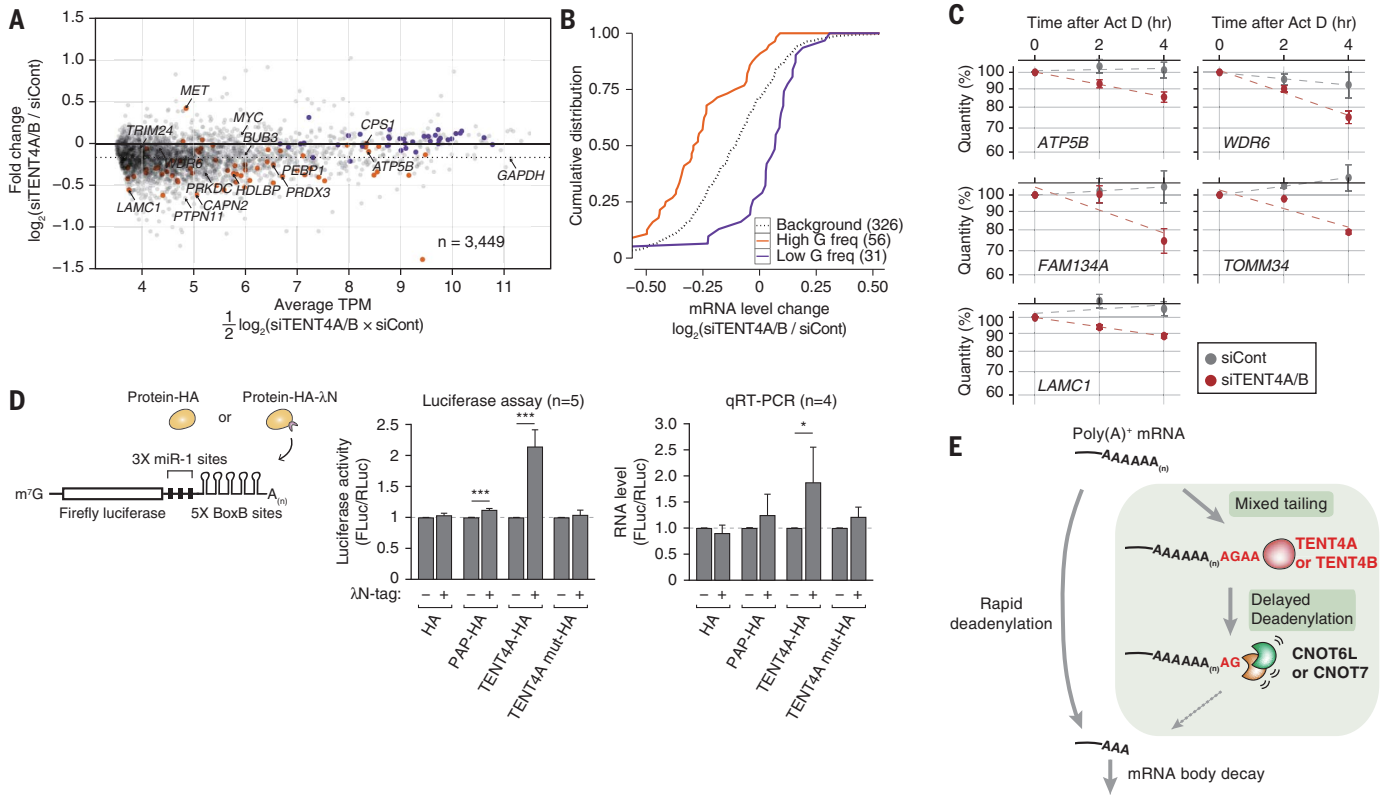

Fig. 4. Mixed tailing by TENT4A and TENT4B stabilizes mRNA. (**A**) Decrease in steady-state mRNA levels after knockdown of TENT4A and TENT4B knockdown ($n = 2$). The dashed horizontal line indicates the median fold change. Labeled mRNAs were validated by quantitative reverse transcription polymerase chain reaction (qRT-PCR) (fig. S4C). TPM, transcripts per million. (**B**) Upon knockdown of TENT4A and TENT4B, mRNA levels of highly guanylated genes ($n = 56$; $P < 0.01$) decreased more than those of genes with low guanylation ($n = 31$; $P < 0.01$). "Background" refers to genes with more than five G and GA counts. Of note, this background cumulative distribution is similar to that of all genes. (**C**) Measurement of half-lives by qRT-PCR ($n = 3$). *GAPDH* (glyceraldehyde phosphate dehydrogenase) was used for normalization. Act D, actinomycin D. (**D**) Tethering experiments. (Left) Experimental scheme. (Right) Reporter protein and mRNA levels were determined by luciferase assays and qRT-PCR, respectively. *$P < 0.05$, ***$P < 0.0001$; two-sided t test. Error bars indicate SEM. (**E**) Proposed model.

were found with TENT4B-tethered reporters (fig. S7, C and D). Thus, the non-adenosine incorporation of TENT4A and TENT4B may be important for mRNA stabilization, although this experiment does not rule out the possible contribution of adenylation. Of note, the same enzymology and function were observed in human foreskin fibroblast (HFF) cells (fig. S8). Growth defects were found in TENT4A/B-depleted HeLa and HFF cells (fig. S9), hinting at the physiological importance of TENT4/B-dependent mRNA tailing (*27*–*29*).

The mRNA tail is thought to be a pure stretch of As, with little informational content except for its length. In this study, we demonstrate that TENT4A and TENT4B generate specialized tails that protect mRNAs from active deadenylation (Fig. 4E). The protective effect may be attributed to both adenylation and mixed tailing. We focused on the impact of non-adenosines added by TENT4A and TENT4B and discovered the considerable stalling effect. The wide range of mRNA destabilization in TENT4A/B-depleted cells opens the possibility of multiple mixed tailing events during the mRNA life span. The "not-so-pure" poly(A) tail is constantly remodeled by tailing enzymes and exoribonucleases and acts as an additional layer for posttranscriptional regulation, in effect changing the way we think about mRNA tails.

REFERENCES AND NOTES

1. C. J. Norbury, *Nat. Rev. Mol. Cell Biol.* **14**, 643–653 (2013).
2. M. Lee, B. Kim, V. N. Kim, *Cell* **158**, 980–987 (2014).
3. H. Chang, J. Lim, M. Ha, V. N. Kim, *Mol. Cell* **53**, 1044–1052 (2014).
4. O. S. Rissland, C. J. Norbury, *Nat. Struct. Mol. Biol.* **16**, 616–623 (2009).
5. J. Lim *et al.*, *Cell* **159**, 1365–1376 (2014).
6. H. Chang *et al.*, *Mol. Cell* **70**, 72–82.e7 (2018).
7. L. Aravind, E. V. Koonin, *Nucleic Acids Res.* **27**, 1609–1618 (1999).
8. T. E. Mullen, W. F. Marzluff, *Genes Dev.* **22**, 50–65 (2008).
9. C. J. Wilusz, J. Wilusz, *Genes Dev.* **22**, 1–7 (2008).
10. C. Rammelt, B. Bilen, M. Zavolan, W. Keller, *RNA* **17**, 1737–1746 (2011).
11. K. Ogami, R. Cho, S. Hoshino, *Biochem. Biophys. Res. Commun.* **432**, 135–140 (2013).
12. J. Houseley, D. Tollervey, *Cell* **136**, 763–776 (2009).
13. J. LaCava *et al.*, *Cell* **121**, 713–724 (2005).
14. P. Viswanathan, J. Chen, Y. C. Chiang, C. L. Denis, *J. Biol. Chem.* **278**, 14949–14955 (2003).
15. C. Bianchin, F. Mauxion, S. Sentis, B. Séraphin, L. Corbo, *RNA* **11**, 487–494 (2005).
16. N. Henriksson, P. Nilsson, M. Wu, H. Song, A. Virtanen, *J. Biol. Chem.* **285**, 163–170 (2010).
17. H. Wang *et al.*, *EMBO J.* **29**, 2566–2576 (2010).
18. S. Niinuma, T. Fukaya, Y. Tomari, *RNA* **22**, 1550–1559 (2016).
19. Y. B. Yan, *RNA* **5**, 421–443 (2014).
20. H. Yi *et al.*, *Mol. Cell* **70**, 1081–1088.e5 (2018).
21. J. Boele *et al.*, *Proc. Natl. Acad. Sci. U.S.A.* **111**, 11467–11472 (2014).
22. H. Berndt *et al.*, *RNA* **18**, 958–972 (2012).
23. C. Kilchert, S. Wittmann, L. Vasiljeva, *Nat. Rev. Mol. Cell Biol.* **17**, 227–239 (2016).
24. B. Boyraz *et al.*, *J. Clin. Invest.* **126**, 3377–3382 (2016).
25. S. Shukla, J. C. Schmidt, K. C. Goldfarb, T. R. Cech, R. Parker, *Nat. Struct. Mol. Biol.* **23**, 286–292 (2016).
26. H. Sudo, A. Nozaki, H. Uno, Y. Ishida, M. Nagahama, *FEBS Lett.* **590**, 2963–2972 (2016).
27. M. Schmid, B. Küchler, C. R. Eckmann, *Genes Dev.* **23**, 824–836 (2009).
28. D. M. Burns, A. D'Ambrogio, S. Nottrott, J. D. Richter, *Nature* **473**, 105–108 (2011).
29. J. Shin, K. Y. Paek, M. Ivshina, E. E. Stackpole, J. D. Richter, *Nucleic Acids Res.* **45**, 6793–6804 (2017).

ACKNOWLEDGMENTS

We thank members of our laboratory for discussion and technical help, especially H. Yi for CNOT7/6L constructs and E. Kim for plasmid cloning. **Funding:** This work was supported by IBS-R008-D1 of Institute for Basic Science from the Ministry of Science, ICT and Future Planning of Korea (J.L., D.K., Y.-s.L., M.H., M.L., J.Y., H.C., J.S., K.A., and V.N.K.) and BK21 Research Fellowships from the Ministry of Education of Korea (D.K. and J.Y.). **Author contributions:** J.L., D.K., and V.N.K. designed experiments.

J.L., D.K., and M.H. performed biochemical and cell biological experiments. M.L. and J.Y. performed TAIL-seq on model organisms. Y.-s.L. and J.L. carried out computational analyses. J.S. and K.A. provided primary HFF cells. J.L., Y.-s.L., and V.N.K. wrote the manuscript. Y.-s.L. and H.C. provided statistical and technical support. **Competing interests:** The authors declare no competing interests. **Data and materials availability:** Sequenced reads have been deposited in the NCBI Gene Expression Omnibus (GEO) database (accession number GSE116355).

SUPPLEMENTARY MATERIALS

www.sciencemag.org/content/361/6403/701/suppl/DC1
Materials and Methods
Figs. S1 to S9
Tables S1 to S5
References (*30*–*33*)

13 December 2016; resubmitted 17 March 2018
Accepted 10 July 2018
Published online 19 July 2018
10.1126/science.aam5794